PRAMANA
— journal of
physics

Vol. 66, No. 6
June 2006
pp. 1037–1048

Computation of the lateral and axial point spread functions in confocal imaging systems using binary amplitude mask

A M HAMED
Physics Department, Faculty of Science, Ain Shams University Cairo, Egypt
Address for correspondence: Physics Department, Faculty of Education at Sur,
P.O. Box 484, Code Postal 411, Sultanate of Oman
E-mail: amhamed73@hotmail.com

MS received 25 October 2005; revised 6 January 2006; accepted 8 February 2006

Abstract. In this paper, a novel aperture based on Tolardo concept composed of a central clear disc surrounded by a series of black and white (B/W) concentric annuli of equal transmittance is presented. Different apodized apertures of different number of B/W annuli are suggested in order to improve further the three-dimensional resolving power of confocal imaging systems. Both the axial and lateral point spread functions (PSF) and the corresponding irradiances are computed in both cases of conventional and confocal scanning microscopes for the above-mentioned amplitude filters. These results of axial and lateral irradiances are graphically represented by constructing a computer program using MATLAB. The obtained results are compared with that obtained in case of circular, annular, and Martinez-Corral apodized aperture.

Keywords. Confocal imaging; lateral and axial resolutions.

PACS No. 42

1. Introduction

The transverse resolution of the coherent scanning optical microscope (CSOM) is dependent on the apertures of the objective lenses. This microscope [1–5] is composed of two conjugate objective lenses arranged in tandem where the transparent object is located at the common short focus of the objectives. The mechanical scanning of the object is made synchronized with the electronic scanning of the detector in order to construct the image during its scanning. It is usual to mention that the point source and the point detector are basically responsible for the spatial coherence of the illumination and the detection [6–10]. The theory of this confocal microscope showed that the resultant point spread function is calculated as the product of the point spread functions corresponding to both the objective

lenses. The main advantage of this confocal microscope is its ability to give better resolution when compared with the conventional optical microscopes.

Another advantage of the confocal microscope is its ability to suppress the legs of its irradiance distribution. Further improvements of transverse resolution are attained [11–16] due to amplitude modulation designed on the apertures. Hence, most of the reported apodization techniques have been aimed at improving the resolving capability of conventional two-dimensional (2D) imaging system, and therefore improving the transverse resolution [14,15]. However, when dealing with confocal imaging system, it is widely used because of its intrinsic optical sectioning capability of imaging three-dimensional (3D) objects. Recently, many authors have designed pupil filters based on Tolardo concept [17]. Tolardo showed that by subdividing the pupil into a proper number of concentric annular zones with constant transmittance, a band-limited transverse diffraction pattern of any shape may be obtained. His concept of modulation has been further applied for shaping the transverse PSF [16,18,19] and also the axial PSF [20–24]. Consequently, both the transverse and axial resolutions are considered equally important for the three-dimensional imaging.

Recently, different apodization techniques were proposed by many authors. Among these authors, are Cheng and Siu [25] and Siu *et al* [26]. They used the apodization technique to achieve the suppression of the side lobes in the point spread function in confocal scanning system. A combination of high numerical aperture of 1.45 oil immersion lens with super-resolving binary filters has been experimentally used to obtain an effective increase in axial resolution by measuring the full-width-half-maximum (FWHM). Also, a novel high-resolution scanning confocal microscope [25] with high numerical aperture (NA = 1) parabolic mirror objective is investigated.

In this paper, a novel pupil based on Tolardo concept is presented. A great number of black and white concentric equally spaced annuli of $N = 19$ with constant transmittance is considered to compute both the lateral and axial amplitude point spread function (APSF). Also, different arbitrarily selected manipulations of non-equally spaced annuli and hence unequal transmittance may be used in order to improve the resolution. The irradiance distributions of conventional and confocal microscopes are computed using our model of multi-ring aperture of equally spaced annuli. Finally, the obtained results are compared with the corresponding results of the transverse and axial irradiances in the case of Martinez-Corral *et al* [23] and in the case of circular apertures. Also, no equally spaced annuli are investigated by changing the obscuration parameter μ. The obtained theoretical results of the APSF and the corresponding irradiances are plotted using MATLAB [27] and discussed, then followed by a conclusion.

2. Theoretical analysis

Consider the amplitude point spread function (APSF) of a coherent imaging system apodized by a purely absorbing pupil filter. Hence [1], we write

$$h(u, w_{20}) = 2\int_0^1 P(\rho)\exp(-j2\pi w_{20}\rho^2)J_0(2\pi u\rho)\rho\,\mathrm{d}\rho, \tag{1}$$

where $P(\rho)$ is the pupil function, ρ being the normalized radial coordinate in the pupil plane, $u = (\rho_0/\lambda f)r$ corresponds to the transverse radial coordinate expressed in optical units, ρ_0 being the maximum extent of the pupil, f is the focal length of the imaging lens and J_0 denotes the Bessel function of the 1st kind and zero order. $w_{20} = r_{20}/2\lambda f^2$ specifies the amount of defocus measured in units of wavelength and r_{20} is the actual radial distance of the defocused cross-section.

Next, it is convenient to perform the following non-linear mapping in order to separate the axial and transverse distributions.

$$\xi = \rho^2 - 0.5, \quad q(\xi) = P(\rho). \tag{2}$$

Then, eq. (1) becomes

$$h(u, w_{20}) = 2\int_{-0.5}^{0.5} q(\xi)\exp(-j2\pi w_{20}\xi)J_0[2\pi u\sqrt{(\xi + 0.5)}]\mathrm{d}\xi. \tag{3}$$

The axial behavior of the system is obtained from eq. (3), at $u = 0$ as follows:

$$h(0, w_{20}) = \int_{-0.5}^{0.5} q(\xi)\exp(-j2\pi w_{20}\xi)\mathrm{d}\xi = \mathrm{FT}[q(\xi)], \tag{4}$$

where FT is the exact Fourier transform realized by the transformation mentioned in eq. (2).

The transverse behavior is obtained from eq. (3), at $w_{20} = 0$ as follows:

$$h(u, w_{20}) = \int_{-0.5}^{0.5} q(\xi)J_0[2\pi u\sqrt{(\xi + 0.5)}]\mathrm{d}\xi. \tag{5}$$

These reported eqs (1)–(5) by Martinez *et al* are used in the next applications using Martinez-Corral filter.

2.1 *Martinez-Corral filter*

The Martinez-Corral filter consists of a transparent annulus and central clear circular aperture of area less than the area of the annulus. The irradiances are computed from eqs (4) and (5) to obtain these results:

$$I(\text{axial}) = \left[\frac{\sin(\pi w_{20})}{(\pi w_{20})}\right]^2 + \mu^2\left[\frac{\sin(\pi\mu w_{20})}{(\pi\mu w_{20})}\right]^2 - 2\mu\frac{\sin(\pi w_{20})}{(\pi w_{20})}\frac{\sin(\pi\mu w_{20})}{(\pi\mu w_{20})}\cos[2\pi w_{20}(\varepsilon - 0.5)\mu] \tag{6}$$

$$I(\text{transverse}) = \frac{1}{\pi^2\mu^2}\{J_1(2\pi\mu) + \sqrt{(0.5-\varepsilon)}J_1[2\pi\mu\sqrt{(0.5-\varepsilon)}] - \sqrt{0.5 + (1-\varepsilon)\mu}J_1[2\pi\mu\sqrt{0.5 + (1-\varepsilon)\mu}]\}, \tag{7}$$

$$q(\xi) = \text{rect}(\xi) - \text{rect}\left[\frac{\xi + (\varepsilon - 0.5)\mu}{\mu}\right],$$

with $0.5 < \varepsilon < 1$ and $0 < \varepsilon\mu < 0.5$, μ is the obscuration parameter, and ε is the asymmetry parameter.

2.2 *Author's filter*

The aperture under study has a definite number of black and white (B/W) annuli of a certain number of circles $N = 20$, where the center is a clear circular disc, as shown in the figure in ref. [12]. The effective pupil of this aperture is mathematically represented as follows:

$$P(\rho) = \text{circ}(\rho/\rho_0) + \sum_{i=1}^{N} \Delta P_i(\rho), \tag{8}$$

where $\Delta P_i(\rho) = P_{2i+1}(\rho) - P_{2i}(\rho)$ is the difference between any two successive circular apertures representing an annular shape, N is the total number of circles and ρ is the radial coordinate in the aperture plane (u, v).

2.2.1 *Computation of the transverse APSF and its irradiance*

The amplitude impulse response of the considered aperture or the amplitude point spread function (APSF) is computed by operating the Fourier transform upon the aperture represented by eq. (8) to obtain the following equation:

$$h(w) = \frac{2J_1(\alpha_1 r)}{(\alpha_1 r)} + \sum_{i=1}^{N} \left\{ \frac{2J_1(\alpha_{2i+1} r)}{(\alpha_{2i+1} r)} - \frac{2J_1(\alpha_{2i} r)}{(\alpha_{2i} r)} \right\}. \tag{9}$$

where $\alpha_{2i} = (2\pi/\lambda f) w_{2i}$ and $\alpha_{2i+1} = (2\pi/\lambda f) w_{2i+1}$, J_1 is the Bessel function of the 1st order and r is the radial coordinate in the Fourier plane (x, y).

In the case of non-equally spaced annuli, eq. (9) is used in the computations suppressing some annuli where the obscuration parameter has $\mu = 0.7895$ giving the best transverse resolution. It corresponds to the following parameters: central disc of radius $\rho = 1/19$ followed by the dark annulus of $\mu = 15/19 = 0.7898$, then followed by the three remaining white–dark–white annuli. The other extreme value of $\mu = 0.0526$ will give a poorer resolution which corresponds to the following parameters: central disc of radius $\rho = 1/19$ followed by the dark annulus of $\mu = 1/19 = 0.0526$, then followed by 12 B/W annuli.

The transverse irradiance is the modulus square of the amplitude point spread function represented as follows:

$$I_{\text{trans.}}(w) = |h(w)|^2. \tag{10}$$

In the case of confocal imaging systems the irradiance or the image of a point becomes

$$I_{\text{trans.}}(w) = |h(w)|^4. \tag{11}$$

For an aperture composed of a very thin annular shape combined with the transparent central disc, eq. (9) becomes

$$h(w) = \frac{2J_1(\alpha_1 r)}{(\alpha_1 r)} + \sum_{i=1}^{N} J_0(\alpha_{2i+1} r). \tag{12}$$

2.2.2 *Computation of the axial APSF and its irradiance*

The binary filter which is composed of 10 transparent annuli and ten black annuli with a central clear disk in B/W cascaded concentric annular arrangement, as shown in the figure in ref. [23], is represented as follows:

$$q(\xi) = \sum_{i=1}^{N} \text{rect}(\xi - n\mu\xi_0), \tag{13}$$

where ξ_0 is the interval width between any two successive annuli and μ is the obscuration parameter. The 1D Fourier transform is operated upon eq. (13), making use of convolution operations, to get this result for the axial APSF:

$$h(w_{20}) = \sum_{n=-N/2}^{N/2} \frac{\sin(\pi w_{20})}{(\pi w_{20})} \exp(j2\pi n\mu\xi_0 w_{20}). \tag{14}$$

This complex function of the axial APSF can be decomposed into real and imaginary parts as follows:

$$\text{Re}\,al[h(w_{20})] = \sin c(w_{20}) \sum_{n=-N/2}^{N/2} \cos(2\pi n\mu\xi_0 w_{20}), \tag{15}$$

$$\text{Im}[h(w_{20})] = \sin c(w_{20}) \sum_{n=-N/2}^{N/2} \sin(2\pi n\mu\xi_0 w_{20}). \tag{16}$$

The corresponding axial irradiance of the ordinary optical systems is computed by taking the modulus square of the axial APSF to get this result:

$$I_{\text{axial}}(w_{20}) = \sin c^2(w_{20}) \left[\sum_{n=-N/2}^{N/2} \cos(2\pi n\mu\xi_0 w_{20}) \right]^2 \tag{17}$$

since the second summation over sine odd function is vanished. In the case of confocal imaging, the axial irradiance is

$$I_{\text{axial}}(w_{20}) = \sin c^2(w_{20}) \left[\sum_{n=-N/2}^{N/2} \cos(2\pi n \mu \xi_0 w_{20}) \right]^4 . \tag{18}$$

This can be rewritten as follows:

$$I_{\text{axial}}(w_{20}) = \sin c^4(w_{20}) \left[1 + 2 \sum_{n=-N/2}^{N/2} \cos(2\pi n \mu \xi_0 w_{20}) \right]^2 . \tag{19}$$

3. Theoretical results and discussion

The proposed filter of multi-ring aperture of B/W concentric annuli of different obscuration parameter (μ) is used in the calculation of the axial and lateral (transverse) PSF and the corresponding irradiances. Eight graphs representing the transverse PSF are shown in figures 1a–8a. These graphs are plotted using eq. (9). The corresponding irradiances are obtained from eq. (10) and represented as in figures 1b–8b. The graphs of the confocal imaging irradiances are obtained using eq. (11) and the plots are similar to the irradiances shown in figures 1–8 except that the legs of the irradiance distribution are attenuated or suppressed. Our multi-ring arrangement is composed of a central clear disc obstructed by a dark annulus of obscuration parameter (μ) then followed by a sandwich of B/W annuli. Referring to the above results, it is shown that the best transverse resolution is corresponding to the following parameters: central disc of radius $\rho = 1/19$ followed by the dark annulus of $\mu = 15/19 = 0.7898$, then followed by white–dark–white annuli. The result corresponding to this arrangement is shown in figure 1b. In this case, the total number of annuli $N = 19$ and the total normalized radius of the aperture is taken to be unity. It is shown that the transverse resolution is decreased as μ is decreased reaching equally spaced concentric B/W annuli. The improvement of transverse resolution in Martinez filter is at the expense of the appearance of the

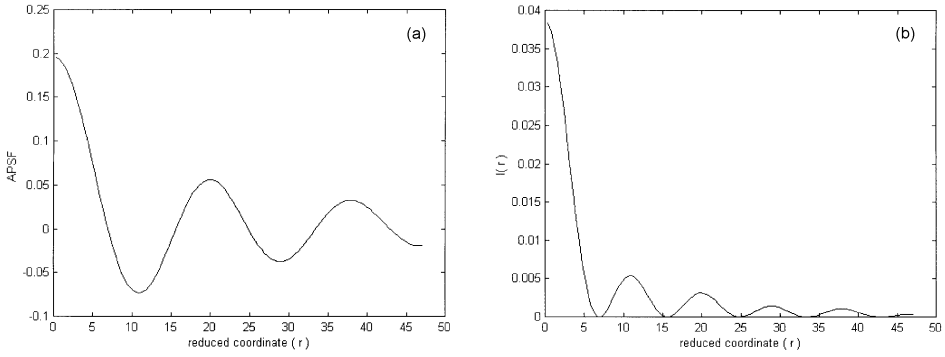

Figure 1. (**a**) Normalized transverse point spread function, where the obscuration parameter = 0.7895. (**b**) Normalized transverse irradiance, where the obscuration parameter = 0.7895.

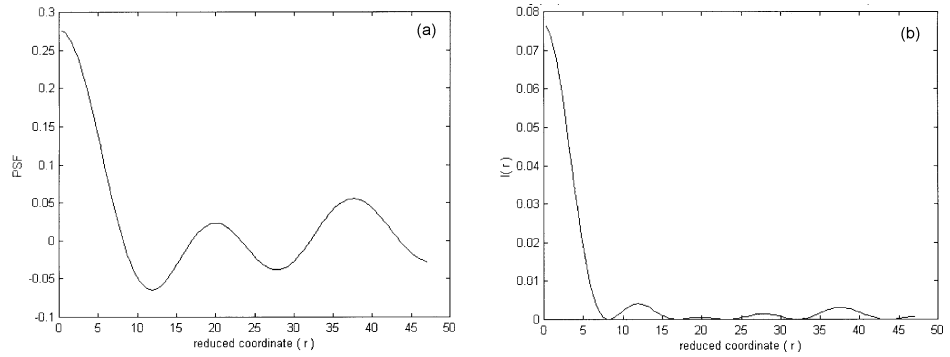

Figure 2. (**a**) Normalized transverse PSF, where the obscuration parameter = 0.6842. (**b**) Normalized transverse irradiance, where the obscuration parameter = 0.6842.

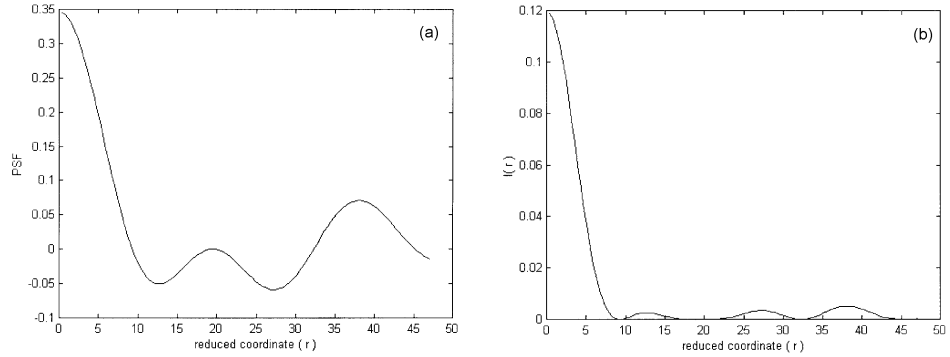

Figure 3. (**a**) Normalized transverse PSF, where the obscuration parameter = 0.5789. (**b**) Normalized transverse irradiance, where the obscuration parameter = 0.5789.

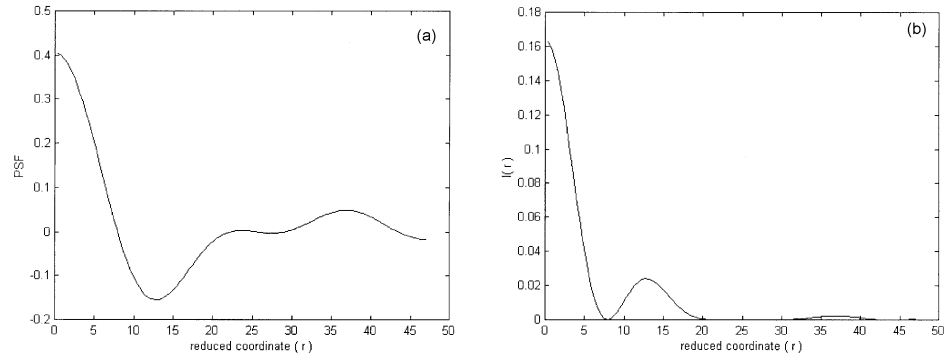

Figure 4. (**a**) Normalized transverse PSF, where the obscuration parameter = 0.4737. (**b**) Normalized transverse irradiance, where the obscuration parameter = 0.4737.

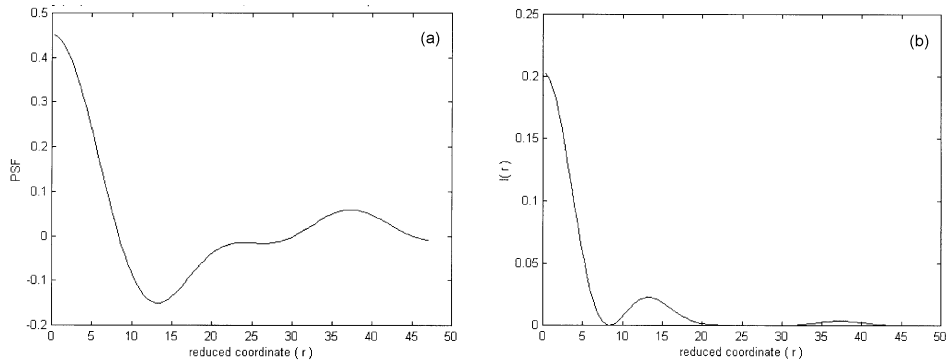

Figure 5. (**a**) Normalized transverse PSF, where the obscuration parameter = 0.3684. (**b**) Normalized transverse irradiance, where the obscuration parameter = 0.3684.

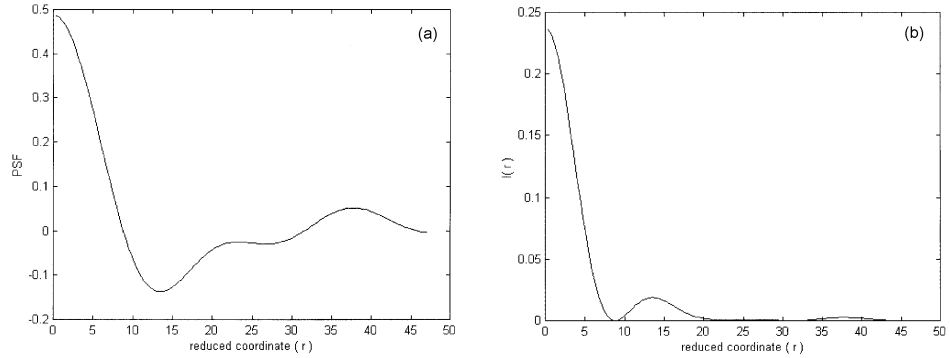

Figure 6. (**a**) Normalized transverse PSF, where the obscuration parameter = 0.2632. (**b**) Normalized transverse irradiance, where the obscuration parameter = 0.2632.

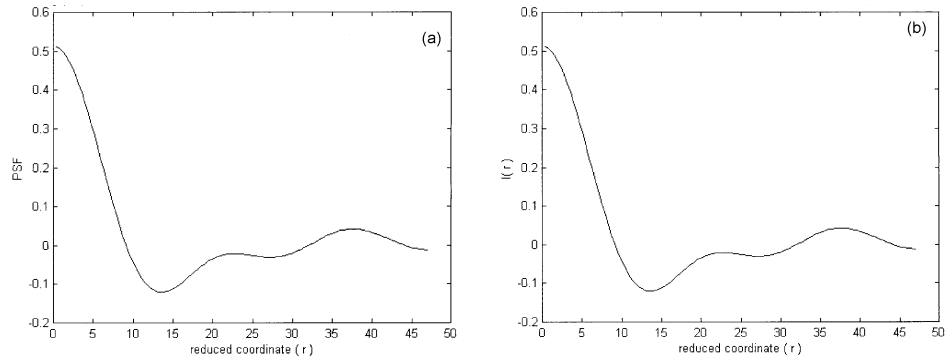

Figure 7. (**a**) Normalized transverse PSF, where the obscuration parameter = 0.1579. (**b**) Normalized transverse irradiance, where the obscuration parameter = 0.1579.

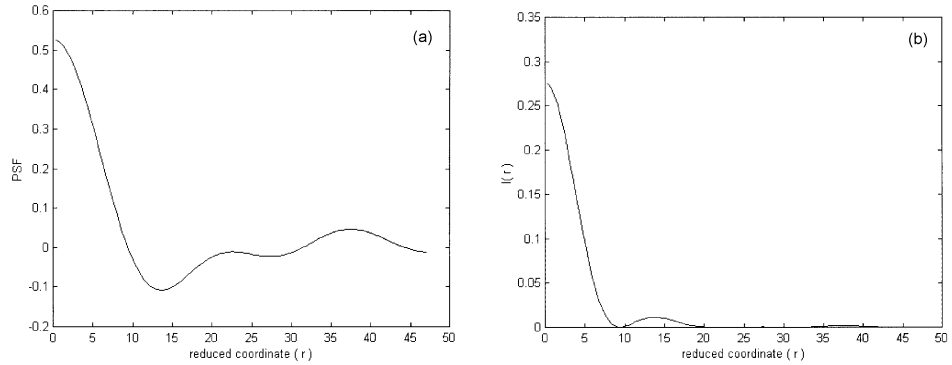

Figure 8. (**a**) Normalized transverse PSF, where the obscuration parameter = 0.0526. (**b**) Normalized transverse irradiance, where the obscuration parameter = 0.0526.

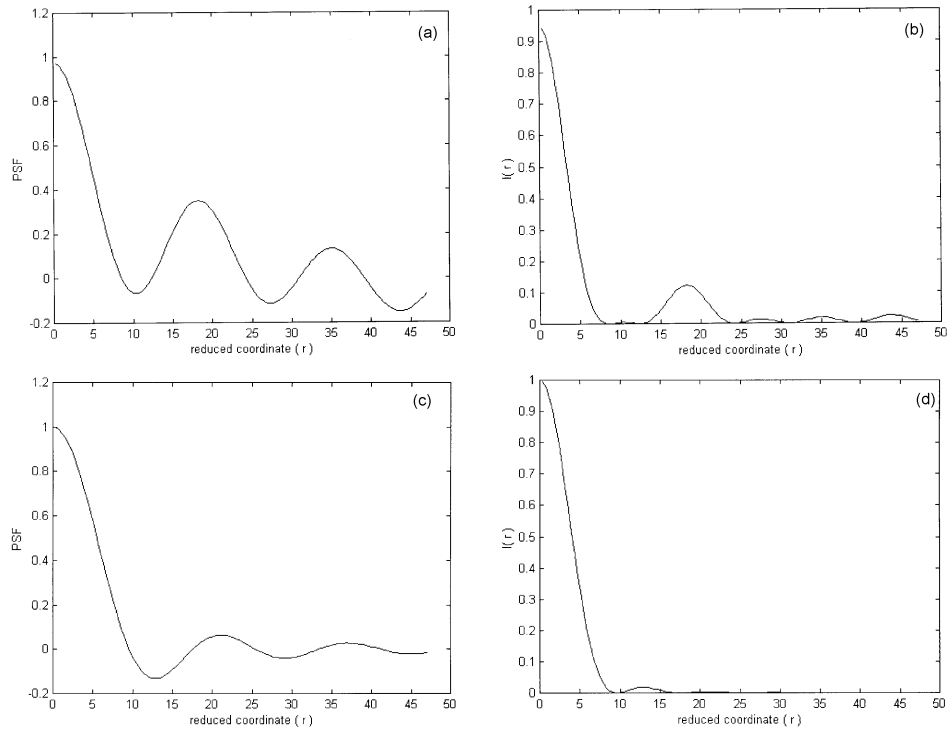

Figure 9. (**a**) Normalized transverse PSF for Martinez filter. (**b**) Normalized transverse irradiance for Martinez filter. (**c**) Normalized transverse PSF for circular aperture. (**d**) Normalized transverse irradiance for circular aperture.

legs of the diffracted irradiance while only one leg of low height is appeared as in figure 8b using our filter. Another advantage of our multi-ring arrangement lies in its gain in intensity. The Martinez-Corral transverse PSF and its corresponding irradiances are plotted in figures 9a and 9b. The axial irradiance is obtained using

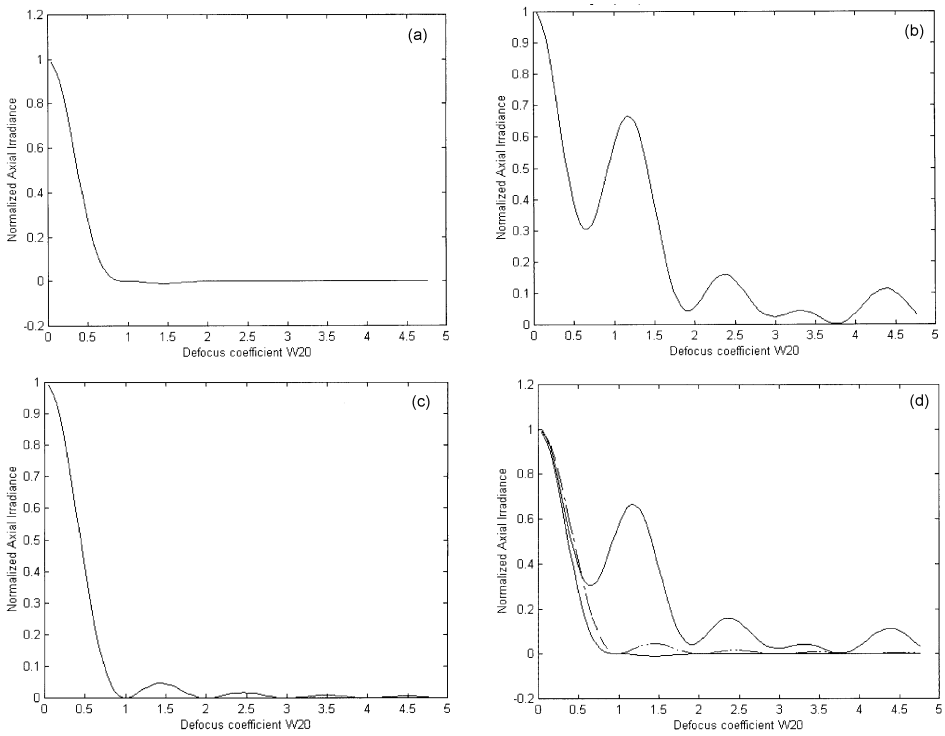

Figure 10. (**a**) Normalized axial irradiance for B/W concentric annuli. (**b**) Normalized axial irradiance for Martinez filter. (**c**) Normalized axial irradiance for clear circular aperture. (**d**) Normalized axial irradiance for B/W annuli, Martinez filter and circular aperture.

eq. (17) and represented as in figure 10a. Another plot corresponding to Martinez filter is made using eq. (6) where $\mu = 0.7$ as shown in figure 10b. Also, a separate curve of irradiance distribution for circular aperture is appeared as in figure 10c. A set of axial irradiances for the different filters and circular aperture are combined and plotted as shown in figure 10d, where the discontinuous curve is set for circular aperture and the curve corresponding to our filter has no legs as compared with Martinez curve which has a dominant distribution outside the central band. It is shown that our axial irradiance curve lies between Martinez curve and circular aperture discontinuous curve. Referring to the results shown in figure 10d our filter has a resolution better than that obtained for the circular curve and less than the Martinez resolution. The advantage of our filter when compared with Martinez filter lies in its suppression of the legs of the axial irradiance and the reasonable gain obtained of the detected intensity. It is shown, referring to the results of the axial PSF for different values of μ, as shown in figures 11a–11d, that as the obscurity parameter is increased the axial resolution is improved. As μ is decreased the axial resolution becomes poorer and the legs of the diffraction pattern will appear. Hence, it is recommended to take greater value of obscuration parameter

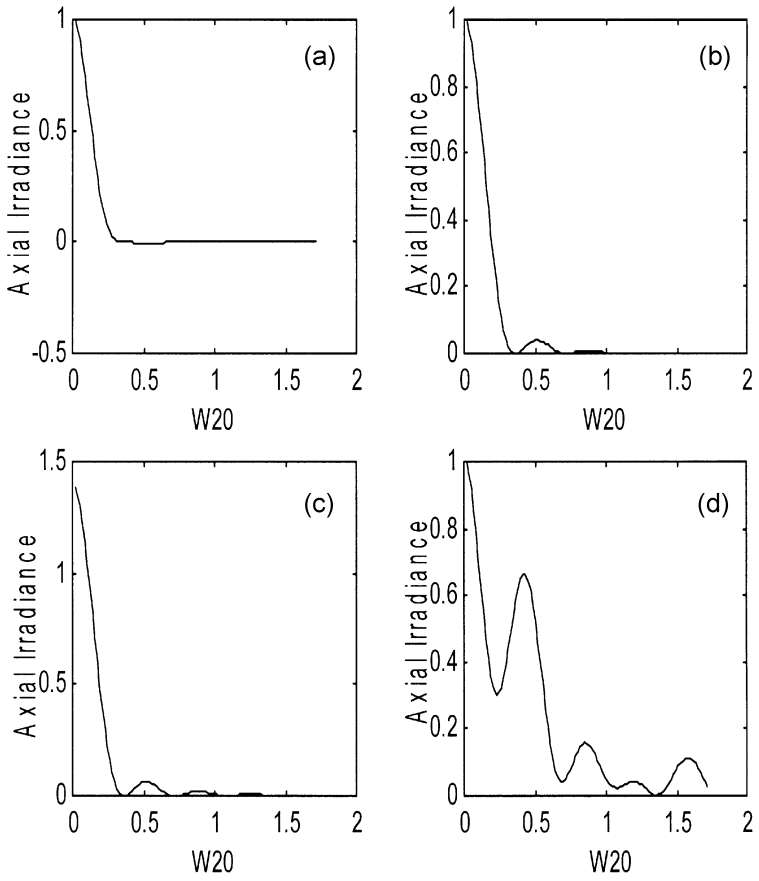

Figure 11. (**a**) Author's axial irradiance, $\mu = 1.0$. (**b**) I-axial, $\mu = 0.8$. (**c**) I-axial, $\mu = 0.5$. (**d**) Martinez axial irradiance.

in order to get better resolution and equally to suppress the legs of the diffraction pattern.

4. Conclusion

The model of multi-ring aperture of B/W concentric annuli is presented. We have computed both the transverse and axial PSF and the corresponding irradiances. The obtained results are compared with the results of Martinez-Corral annular obstruction filter and also compared with the clear circular aperture. It is concluded that the obtained transverse resolution is better than that obtained for circular aperture while it is less than that obtained for Martinez filter. It is found that the transverse resolution is dependent upon the obscuration parameter μ and is improved for greater values of μ in the case of our filter. Hence, further improvement of resolution may be attained in the case of non-equally spaced annuli which is

dependent upon the obscuration parameter μ. The axial resolution corresponding to our filter lies between the Martinez resolution and circular aperture resolution. In the case of Martinez filter the legs of the irradiance distribution are appeared while in the case of our filter complete suppression of the legs is occurred for $\mu = 1.0$ making our amplitude filter better than the Martinez filter.

References

[1] C J R Sheppard and A Choudhary, *Opt. Acta* **24**, 1051 (1977)
[2] C J R Sheppard and T Wilson, *J. Microscopy* **114**, 179 (1978)
[3] T Wilson, *Appl. Phys.* **22**, 119 (1980)
[4] C J R Sheppard, *Optik* **48**, 329 (1977)
[5] C J R Sheppard and T Wilson, *Opt. Acta* **25**, 315 (1978)
[6] A M Hamed, *Opt. Laser Technol.* **22**, 137 (1990)
[7] A M Hamed, *Opt. Laser Technol.* **29**, 93 (1997)
[8] J D Gaskill, *Linear systems, Fourier transform and optics* (Wiley, New York, 1978)
[9] J W Goodmann, *Introduction to Fourier optics and holography* (McGraw-Hill Co., New York, 1968)
[10] R N Bracewell, *Fourier transform and its applications* (McGraw-Hill Co, New York, 1966)
[11] J J Clair and A M Hamed, *Optik* **64**, 133 (1983)
[12] A M Hamed and J J Clair, *Optik* **64**, 277 (1983)
[13] A M Hamed and J J Clair, *Optik* **65**, 209 (1983)
[14] A M Hamed, *Opt. Laser Technol.* **16**, 93 (1984)
[15] A M Hamed, *Optik* **107**, 161 (1998)
[16] C J R Sheppard and Z S Hegedus, *J. Opt. Soc. Am.* **A5**, 643 (1988)
[17] G Toraldo di Francia, *Atti Fond. Giorgio Ronchi* **7**, 366 (1952)
[18] Z S Hegedus and V Sarafis, *J. Opt. Soc. Am.* **A3**, 1892 (1986)
[19] T R M Sales and G M Morris, *J. Opt. Soc. Am.* **A14**, 1637 (1997)
[20] T R M Sales and G M Morris, *Opt. Commun.* **156**, 227 (1998)
[21] C J R Sheppard, G Calvert and M Wheatland, *J. Opt. Soc. Am.* **A15**, 849 (1998)
[22] H Wang and F Gan, *Appl. Opt.* **40**, 5668 (2001)
[23] M Martinez-Corral, M T Caballero, E H K Stelzer and J Swonger, *Opt. Express* **10**, 98 (2002)
[24] C M Blanc and S W Hell, *Opt. Express* **10**, 893 (2002)
[25] L Cheng and G G Siu, *Meas. Sci. Technol.* **2**, 198 (1991)
[26] G G Siu, L Cheng and K S Chang, *J. Phys.* **D27**, 459 (1994)
[27] O Hanselman and B Littlefield, *Mastering MATLAB 5* edited by M Horton (Upper Saddle River, New Jersey 07458, 1998) Ch. 22, p. 238